Investigation of a spectral formulation for radiative heat transfer in one-dimensional fires and combustion systems

Siaka Dembele, Jennifer X. Wen*

Combustion and Fire Modelling Group, School of Mechanical, Aeronautical and Production Engineering, Kingston University, Roehampton Vale, Friars Avenue, London SW15 3DW, UK

Abstract

The radiative heat transfer in variable concentration, non-isothermal and sooty combustion products is investigated with a correlated-k gas method and discrete ordinates technique for the solution of equation of transfer. The spectrally formulated model is an approach for predicting radiative intensities and fluxes in mixtures of gaseous products (H_2O, CO_2, CO) and scattering soot particles. The reliability of this approach for fire and combustion applications is analysed by comparing its predictions with some theoretical results and measured radiative intensities for a natural gas flame. Use of this model for more accurate calculations and evaluation of simplified fire and combustion radiation models, are among its main advantages. © 2000 Elsevier Science Ltd. All rights reserved.

1. Introduction

Radiative heat transfer analysis in fires and combustion systems is a subject of major concern. In these systems, evaluation of the radiative intensities and heat flux distributions is of great interest. For example in pool fire studies, the determination of radiative heat feedback is essential for the calculation of the mass burning rate. For such fires the heat transferred from the flame to the burning fuel surface can be divided into conductive, convective and radiative terms [1,2]. However it is now well established, from literature works, with few exception, that hydrocarbon pool fires of diameter larger than about 0.3 m, which are the ones of practical interest, burn in radiatively dominated regime. For the radiation calculations of such

pool fires or combustion systems in general, many studies have assumed a flame constant grey absorption coefficient, uniform temperature and concentration distribution in the combustion products. These assumptions have led to some important errors [3,4]. Thus, realistic radiative models for combustion system investigations should take into account the non-grey or spectral dependency nature of the combustion products. The non-uniformity of the temperature and species distributions should also be considered. The accuracy of the calculations will mainly depend on the gas model used and the actual radiative transfer equation (RTE) solution method. Since the spectral absorption coefficients of real combustion gases are highly variable within the vibration-rotation bands and difficult to obtain, various levels of approximations have been developed to quantify the gas properties within certain spectral interval Δv. One of the main differences between these approximations are the width of the spectral interval used, varying from line-by-line to entire wide band models. It is not viable for the

---

* Corresponding author. Tel.: +44-181-547-7836; fax: +44-181-547-7992.

E-mail address: j.wen@kingston.ac.uk (J.X. Wen).

Nomenclature

ck	correlated-k gas model
d	soot particle diameter, μm
DOM	discrete ordinates method
$f(k)$	k-distribution function in gas model
f_v	soot particles volume fraction
g_j	jth quadrature point in ck method
$g(k)$	cumulative distribution function in gas model
I	total intensity of radiation, W/(m² sr)
I_ν	spectral intensity of radiation, W/(m² sr cm⁻¹)
$k, k(\nu)$	gas spectral absorption coefficient, atm⁻¹ cm⁻¹ or atm⁻¹ m⁻¹
$\tilde{k}$	imaginary part of the soot particle refraction index
$\overline{k_\nu}$	mean line-intensity to spacing ratio, atm⁻¹ cm⁻¹
K	volumetric spectral absorption coefficient, m⁻¹ or cm⁻¹
L	thickness of the medium, m
m	discrete direction in DOM
$\tilde{n}$	real part of the soot particle refraction index
NBS	narrow band statistical
N_d	number of discrete directions in DOM
N_q	number of quadrature points in ck gas model calculations
P	scattering soot particle phase function, or gases total pressure, atm
q	local heat transfer rate per unit area, W/m²
RTE	radiative transfer equation
T	temperature, K, transmissivity
W_m	weight of a discrete direction m in DOM
x	position variable, m

Greek symbols

α	size parameter $= \pi d/\lambda$
$\overline{\gamma_\nu}$	mean half-width of the absorbing lines inside $\Delta\nu$, cm⁻¹
$\overline{\delta_\nu}$	equivalent line spacing, cm⁻¹
ε	emissivity
θ	polar angle measured from x axis
λ	wavelength
μ	direction cosine $= \cos\theta$
ν	wavenumber, cm⁻¹
$\Delta\nu$	wavenumber range, cm⁻¹
ϱ	reflectivity $= 1 - \varepsilon$
σ	soot spectral scattering coefficient, m⁻¹
χ	molar fraction
ω_j	weight of a quadrature point g_j in ck method
Ω	solid angle, sr

Subscripts

b	blackbody
CO_2	carbon monoxide
CO_2	carbon dioxide
g	relative to absorbing/emitting gases
H_2O	water vapour
j	relative to the jth quadrature point in ck method
m	relative to a discrete direction m in DOM
s	relative to soot particles
ν	spectral value

Superscripts

−	spectrally averaged
'	incoming direction

line-by-line method, $\Delta\nu \cong 0.0002$–0.02 cm⁻¹, although exact, to be used in practical engineering applications because of the enormous amount of computational time it requires. The extensively used wide band model, $\Delta\nu \cong 100$–1000 cm⁻¹, developed by Edwards [5] is based on the assumption of an exponential line distribution and a constant pressure broadening parameter for the wide band. Although this last approach reduces the computational time and can be applied to non-homogeneous and non-isothermal gases, with a reasonable loss of accuracy, its main shortcoming is the lack of more spectral information, which can deform the radiation intensity profiles [6]. Similar deficiencies, i.e. lack of spectral information, are also present in models such as the weighted-sum-of grey gases [7] which allow the calculation of total or wavelength

integrated radiative quantities such as emissivities, intensities, and heat fluxes. The deficiencies of these models have prompted the development of the more sophisticated spectral narrow band statistical (NBS) models. NBS models describe the radiative properties of a homogeneous and isothermal gaseous media in terms of mean transmissivities averaged over spectral interval $\Delta\nu \cong 5$–50 cm⁻¹. The two most extensively used models, of such type were developed by Goody [8] and Malkmus [9]. The basic difference between the two NBS models consists of the line intensity distribution function. An exponential decay is adopted in Goody's formulation, whereas Malkmus used an exponential tailed s⁻¹ distribution of line intensities, which accounts for more low intensity lines in the band and is more accurate for certain bands. For the compu-

tation of turbulent combustion problems with computational fluid dynamics (CFD) methods, some investigators have presented "faster" NBS based models, e.g., FASTNB of Yan and Holmstedt [10]. However, NBS approach presents two major disadvantages. Firstly, for non-homogeneous and non-isothermal media, they require further approximations such as Curtis–Godson or Lindquist–Simmons, that may lead to inaccurate results [11]. Secondly, the fact that they describe the properties of the mixture of gas and non-scattering particles in terms of transmissivity, make them difficult to use for radiative transfer including scattering particles. An alternative method, which does not have these disadvantages, are the spectral k and correlated-k (ck) methods, studied for atmospheric applications by Goody and Yung [8], but little used in combustion applications. The ck approach is based on the cumulative distribution of the absorption coefficient, and can be applied to homogeneous/non-homogeneous, isothermal/non-isothermal and scattering gas/particle mixtures. Dembele et al. [12] have used the method for isothermal water sprays application. Moreover, in most previous studies of radiative transfer in combustion systems, the scattering of soot particles was assumed negligible in comparison to their absorption (e.g. [13–15]). Although this assumption, valid in many situations, leads to major simplifications in the problem and can save valuable computing time, there is a need for more comprehensive models which incorporate the scattering effects of soot particles. Thus, one can quantify the influence of neglecting scattering effects on the calculated radiative intensities and heat flux profiles of practical combustion systems and accidental fires. In the current study, the spectral ck method is coupled with discrete ordinate method (DOM) for radiative equation solution, to investigate radiative heat transfer in non-homogeneous and non-isothermal combustion products consisting of H_2O, CO_2, CO and scattering soot particles. The first goal is to calculate more accurately the radiative quantities such as intensities, heat fluxes and source terms in combustion systems with a reasonable compromise between accuracy and CPU time. The second objective is to develop a tool capable of evaluing simplified radiative models i.e. non-spectral and non-scattering based, used in fire and combustion applications.

2. Theoretical formulation

2.1. Equations of radiative transfer

We will consider in this study the radiative heat transfer between two parallel absorbing/reflecting surfaces in planar geometry (Fig. 1). This one-dimensional radiative transfer assumption has been used by some

authors [15,16] for large pool fires. It can also be suitable for some other combustion systems. Studies of other geometries, do not formally involve major difficulties and are based on the same procedure presented here. The participating medium between the two surfaces is non-uniform in temperature, with variable concentration of soot particles and gaseous products of combustion.

The spectral radiative transfer equation (RTE) for azimuthally symmetric condition is expressed by the following [17]:

$$\mu \frac{\partial I_v(x,\mu)}{\partial x} = -\left[K_{vg}(x) + K_{vs}(x) + \sigma_{vs}(x)\right]I_v(x,\mu)$$
$$+ \left[K_{vg}(x) + K_{vs}(x)\right]I_{bv}\left[T(x)\right]$$
$$+ \frac{\sigma_{vs}(x)}{2} \int_{-1}^{1} P(\mu,\mu')I_v(x,\mu')\,d\mu' \qquad (1)$$

where I is the intensity, $\mu = cos\,\theta$, θ is the polar angle measured from the x axis and $K_{vg} = K_{vH_2O} + K_{vCO_2} + K_{vCO}$ is the spectral absorption coefficient of the gaseous mixture.

In the particular Rayleigh region ($\alpha << 1$ and $\alpha|\tilde{n} - 1| << 1$) typical to soot particles, the phase function is expressed as [17]:

$$P(\mu,\mu') = 1 + \frac{1}{8}(3\mu^2 - 1)(3\mu'^2 - 1). \qquad (2)$$

The soot particles spectral absorption and scattering coefficients are calculated based on Mie theory [18], which provides the following equations in the Rayleigh limit:

$$K_{vs} = \frac{36\alpha f_v \tilde{n}\tilde{k}}{d\left[\left(\tilde{n}^2 - \tilde{k}^2 + 2\right)^2 + 4\tilde{n}^2\tilde{k}^2\right]} \qquad (3)$$
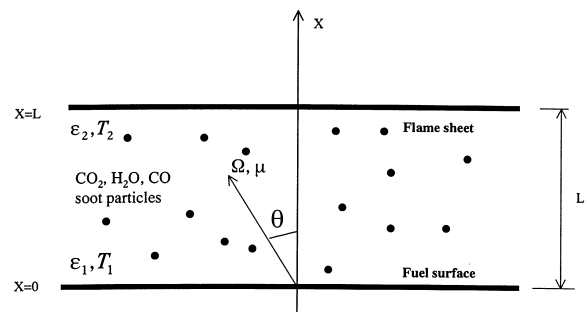
Fig. 1. Typical physical system considered: radiative transfer between the flame and fuel surface.

$\sigma_{vs} =$

$$\frac{4\alpha^4 f_v}{d} \frac{\left[\left(\tilde{n}^2 - \tilde{k}^2 - 1\right)\left(\tilde{n}^2 - \tilde{k}^2 + 2\right) + 4\tilde{n}^2\tilde{k}^2\right]^2 + 36\tilde{n}^2\tilde{k}^2}{\left[\left(\tilde{n}^2 - \tilde{k}^2 + 2\right)^2 + 4\tilde{n}^2\tilde{k}^2\right]^2}.$$

(4)

Spectral values of $\tilde{n}(v)$ and $\tilde{k}(v)$ used in this work are obtained from Lee and Tien [19]. The discrete ordinates method [20,21] is based on the separation of the angular dependence from the spatial dependence of the intensity in the RTE. This is achieved by choosing a set of discrete directions spanning in the angular range of 4π. The method is easy to be incorporated into CFD calculations and is computationally faster in some situations than the discrete transfer method [22]. For the one-dimensional slab considered here, as shown by Eq. (1), the integration reduces to quadrature on $[-1,1]$ interval. A discrete ordinates Gauss–Legendre angular quadrature scheme on $[-1,1]$ is selected in this work. It is important to underline that there is no optimum quadrature for all situations.

By the discrete ordinates technique the governing equations are evaluated for a discrete number of directions m of weight W_m, and the integral term in Eq. (1) is replaced by a numerical Gauss–Legendre quadrature:

$$\mu_m \frac{\partial I_{vm}(x)}{\partial x} = -\left[K_{vg}(x) + K_{vs}(x) + \sigma_{vs}(x)\right]I_{vm}(x)$$

$$+ \left[K_{vg}(x) + K_{vs}(x)\right]I_{bv}\left[T(x)\right]$$

$$+ \frac{\sigma_{vs}}{2}\sum_{m'=1}^{Nd} W_{m'}P\left(m,m'\right)I_{vm'}(x).$$

(5)

To solve Eq. (5), the following diffusely reflecting boundary conditions are set, respectively at $x = 0$ and $x = L$:

$$I_{vm} = \varepsilon_1 I_{bv}[T_1] + 2(1 - \varepsilon_1)\sum_{m'=1,\mu'<0}^{Nd} \mu_{m'}w_{m'}I_{vm'}(x),$$

(6)

$\mu_m > 0$ at $x = 0$

$$I_{vm} = \varepsilon_2 I_{bv}[T_2] + 2(1 - \varepsilon_2)\sum_{m'=1,\mu'>0}^{Nd} \mu_{m'}w_{m'}I_{vm'}(x),$$

(7)

$\mu_m < 0$ at $x = L$

The set of differential equations (5)–(7) is solved by selecting a spatial discretization scheme. For non-grey and non-gaseous media these solutions can be found in an iterative manner without major difficulties [23]. However, because the non-grey gases and scattering

soot particles simultaneously interact with radiation, two major difficulties are encountered in solving this set of equations.

Firstly, except through the highly time consuming line-by-line procedure, the gases spectral absorption coefficient K_{vg} in Eq. (5), varying in a complex manner with frequency, cannot be used in practice. It is important to note that for CO_2 and H_2O in the infrared region, there are about 10^5–10^6 spectral lines and the RTE should be solved a similar number of times.

Secondly, because of the in-scattering term, it is a difficult task to use reasonable CPU time gas models such as the transmissivity formulated NBS method even with the integrated RTE. Scattering problems cannot be treated by band models.

Without the in-scattering term, this can be easily achieved [10,24].

Gaseous models based on absorption coefficient concept, such as the k or ck distribution methods are an alternative to overcome these drawbacks with acceptable CPU times.

2.2. Gases modelling with the correlated-k approach

More details and deeper understanding concerning k and ck distribution methods may be found in Goody and Yung [8]. Here we will only outline the basic definitions that are essential for understanding our analysis. The k and ck methods have been widely used in atmospheric problems [8,25]). The former is suitable for homogeneous and isothermal gases problems while the latter is the extension to non-homogeneous and non-isothermal cases. They offer the advantage to be formulated in terms of absorption coefficient and are therefore compatible with any method of solution of the RTE. The k and ck techniques can be used for scattering problems, contrary to band models, with reasonable CPU time. The concept of ck approach is to transform frequency integration, into integration over absorption coefficient. Recently, Lacis and Oinas [25] reported a detailed testing of the ck method based on Malkmus NBS model [9] parametric fits, and this approach will be adopted in this work. The method is based on the cumulative distribution function $g(k)$, in the form:

$$g(k) = \int_0^k f(k')\,dk'.$$

(8)

$g(k)$ is a monotonically increasing and smooth function in k space, with an inverse $k(g) = g^{-1}(k)$. $k(v)[\text{atm}^{-1}\text{m}^{-1}]$ is related to the volumetric gas absorption coefficient $K_{vg}[\text{m}^{-1}]$ by $K_{vg} = \chi_{H_2O}Pk_{H_2O}(v) + \chi_{CO_2}Pk_{CO_2}(v) + \chi_{CO}Pk_{CO}(v)$, P and χ are the total pressure and molar fraction, respectively. In Eq (8), $f(k)$ is the k-distribution function obtained

by inverse Laplace transform of the Malkmus NBS [9] model transmissivity [25,26] by:

$$f(k) = \frac{1}{k}\sqrt{\frac{\overline{k_\nu \gamma_\nu}}{\pi \overline{k_\nu}\overline{\delta_\nu}}}\exp\left[\frac{\overline{\gamma_\nu}}{\overline{\delta_\nu}}(2 - k/\overline{k_\nu} - \overline{k_\nu}/k)\right], \qquad (9)$$

with a peak value at:

$$k_{max} = \left(\overline{k_\nu}/(4\overline{\gamma_\nu}/3\overline{\delta_\nu})\right)\left(\sqrt{\left(4\overline{\gamma_\nu}/3\overline{\delta_\nu}\right)^2 + 1} - 1\right). \qquad (10)$$

In this work, the parameters $\overline{k_\nu}$ and $\overline{\delta_\nu}$ for H_2O, CO_2 and CO are taken from Soufiani and Taine [27]. These parameters, dependent on temperature, are tabulated for a set of spectral intervals, $\Delta\nu = 25$ cm^{-1} wide, centred on a frequency ν characterised by a significant absorption. The temperature and spectral ranges considered are respectively 300–2900 K and 150–9300 cm^{-1}, i.e, 1 to 66 μm. The parameters $\overline{\gamma_\nu}$ of the considered absorbing gases are given by [27]:

$$\overline{\gamma}_{\nu H_2O} = \frac{P}{P_s}\left\{0.462\chi_{H_2O}\left(\frac{T_s}{T}\right) + \left(\frac{T_s}{T}\right)^{0.5}[0.079(1 \right.$$
$$\left. - \chi_{CO_2} - \chi_{O_2}) + 0.106\chi_{CO_2} + 0.036\chi_{O_2}]\right\}, \quad (11)$$

$$\overline{\gamma}_{\nu CO_2} = \frac{P}{P_s}\left(\frac{T_s}{T}\right)^{0.7}\{0.07\chi_{CO_2} + 0.058(1 - \chi_{CO_2} - \chi_{H_2O}) $$
$$+ 0.1\chi_{H_2O}\}, \qquad (12)$$

$$\overline{\gamma}_{\nu CO} = \frac{P}{P_s}\left\{0.075\chi_{CO_2}\left(\frac{T_s}{T}\right)^{0.6} + 0.12\chi H_2O\left(\frac{T_s}{T}\right)^{0.82}\right.$$
$$\left. + 0.06\left(\frac{T_s}{T}\right)^{0.7}(1 - \chi_{CO_2} - \chi H_2O)\right\}. \qquad (13)$$

In these equations, $P_s = 1$ atm and $T_s = 296$ K. P and T are the total pressure and temperature of the gases, respectively.

In the *ck* formulation, the spectrally averaged value of any function of the absorption coefficient $\mathscr{R}[k(\nu)]$ can be written as:

$$\overline{\mathscr{R}[k(\nu)]} = \frac{1}{\Delta\nu}\int_{\Delta\nu}\mathscr{R}[k(\nu)]\,d\nu = \int_0^1 \mathscr{R}[k(g)]$$
$$dg \cong \sum_{j=1}^{Nq}\omega_j \mathscr{R}[k(g_j)]. \qquad (14)$$

Because of the smooth variation in g space, contrary to frequency ν space, integration on [0,1] interval in Eq. (14) can be approximated by a quadrature formula

for practical use of the *ck* method. In this work $N_q = 10$ classical Gaussian quadrature points g_j of weight ω_j [28] are used, and this number was found to be sufficient for atmospheric pressure problems [8,25]. A preliminary investigation for the combustion configurations encountered here, has shown that the accuracy of the results presented in this work did not change significantly when more than 10 points were used.

Calculations of $k(g_j)$ values are based on a Newton–Raphson procedure (k_{max} given by Eq. (10) is the starting point) which is only based on $\overline{k_\nu}$ and $\overline{\delta_\nu}$ values [25]. The transmissivity of a non-homogeneous and non-isothermal absorbing gas column, divided into M discrete homogeneous and isothermal paths of length L_i, and molar fraction χ_i is given by:

$$\overline{T_\nu} = \sum_{j=1}^{N_q}\omega_j \exp\left(-\sum_{i=1}^{M}k_i(g_j)\chi_i PL_i\right). \qquad (15)$$

2.3. Calculation of spectrally averaged radiative intensities and heat fluxes

To obtain the spectrally averaged intensity, Eq. (5) is averaged on each spectral interval $\Delta\nu$, i.e. the operator $\frac{1}{\Delta\nu}\int_{\Delta\nu}(\ldots)\,d\nu$ is applied.

Using the properties of Eq. (14) we obtain:

$$\mu_m\frac{\partial I_{jm}(x)}{\partial x} = -\left[K_{jg}(x) + K_{\nu s}(x) + \sigma_{\nu s}(x)\right]I_{jm}(x)$$
$$+ \left[K_{jg} + K_{\nu s}\right]\overline{I_{b\nu}}\left[T(x)\right]$$
$$+ \frac{\sigma_{\nu s}}{2}\sum_{m'=1}^{N_d}w_{m'}P(m,m')I_{jm'}(x). \qquad (16)$$

where $K_{jg} = \chi_{H_2O}Pk_{H_2O}(g_j) + \chi_{CO_2}Pk_{CO_2}(g_j) + \chi_{CO}Pk_{CO}(g_j)$ and $\overline{I_{b\nu}}$ is the smoothed blackbody intensity at the spectral interval $\Delta\nu$ centre. The soot particles properties are slowly varying within $\Delta\nu$ and therefore assumed constant for each spectral interval. For the calculations here, the width of $\Delta\nu$ is 25 cm^{-1}, following the gas parameters database for the parameters $\overline{k_\nu}$ and $\overline{\delta_\nu}$ [27]. The spatial discretization to solve the set of differential equations (16) is performed by subdividing the medium in control volumes. Then by integrating each equation over the control volume, assuming a constant source term S_{jm} at the volume centre, the following relation is found:

$$I_{jm}(x) = I_{jm}^*\exp\left(-\beta_j x/\mu_m\right) + \frac{S_{jm}}{\beta_j}\left[1 - \exp\left(-\beta_j x/\mu_m\right)\right], \qquad (17)$$

where

$$S_{jm} = \left[K_{jg} + K_{vs}\right]\overline{I_{bv}}\left[T(x)\right] + \frac{\sigma_{vs}}{2}\sum_{m'=1}^{N_d} w_{m'} P(m,m') I_{jm'}(x)$$

and $\beta_j = K_{jg}(x) + K_{vs}(x) + \sigma_{vs}(x)$. I^*_{jm} is the initial intensity at the entrance face of the control volume. $I_{jm}(x)$ is the resultant intensity after a distance x crossed from the entrance face of the control volume by the intensity I^*_{jm}. Knowing the initial intensity at the entrance face of the control volume and the crossed distance, the intensity can be calculated at both the central grid point and the exit face of volume. The procedure starts with the boundary values and is repeated from one volume to the neighbouring one.

Once the intensities $I_{jm}(x)$ are found, the spectrally averaged intensity $\overline{I_{vm}}(x)$ is expressed by:

$$\overline{I_{vm}}(x) = \frac{1}{\Delta v}\int_{\Delta v} I_{vm}(x)\,dv = \sum_{j=1}^{N_q}\omega_j I_{jm}(x). \tag{18}$$

From the spectral values, the total intensities are calculated by integration:

$$I_m(x) = \sum_{\text{all }\Delta v}\overline{I_{vm}}(x)\Delta v. \tag{19}$$

The spectrally averaged and total net radiative heat flux at any location are respectively given by:

$$\overline{q_v}(x) = \sum_{m=1}^{N_d} w_m \mu_m \overline{I_{vm}}(x), \tag{20}$$

$$q(x) = \sum_{\text{all }\Delta v}\overline{q_v}(x)\Delta v. \tag{21}$$

All the radiative quantities, i.e. intensity, heat flux, source term, are evaluated in this work at the central grid-point of each control volume. The radiative source term, $-dq/dx$ in the medium, used for CFD calculations in the energy equation, for combustion systems is obtained by either finite differencing the net fluxes or by the difference between the absorption and emission terms. The former procedure is used here. The source term at the central grid point $i + 1/2$ of the control volume with faces location i and $i + 1$ is given by:

$$-\frac{dq}{dx}\bigg|_{i+1/2} = -\frac{q_{i+3/2} - q_{i-1/2}}{x_{i+3/2} - x_{i-1/2}}. \tag{22}$$

For geometries other than planar, the same procedure can be followed in treating the equations. For multidimensional rectangular or cylindrical geometries, the reader may refer to Carlson and Lathrop [21], or Fiveland [29], for the use of the discrete ordinates method.

3. Results and discussion

3.1. Flame intensities calculations

The accuracy and CPU time of the approach presented in the previous section for radiative transfer calculations in non-homogeneous and non-isothermal gases, is analysed here, for real flame conditions. The experimental data are taken from Ref. [6] for a 750 kW natural gas industrial diffusion flame in a combustion chamber. A narrow probe equipped with a total radiation pyrometer measured the intensities of flame radiation, in a direction perpendicular to the flame axis. Fig. 2 presents measured distributions of the flame parameters at the distance of 0.6 m along the axis, illustrating non-homogeneous and non-isothermal combustion gases.

Calculations with the model, for this non-sooty configuration are performed in a line-of-sight calculation with 38 nodes or supdivisions along the path length. The experimental data were obtained for these same points. Fig. 3 shows the comparison between the measured and calculated total intensities with the current ck approach using Eq. (19). The spectral region accounts for in the ck calculations, the major absorption bands of H_2O, CO_2, CO and range from 1 to 20 μm, i.e 500–9300 cm^{-1} comprising 353 spectral bands of width $\Delta v = 25$ cm^{-1} for H_2O, 96 for CO_2 and 48 for CO. A good agreement is observed between the measured and calculated total intensities. Although the uncertainties on measured intensities are not provided in Ref. [6], for the intensities leaving the flame and reaching the surrounding targets at end-path $x = 1$, the relative difference between the measured and calculated values are within 4.2% in Fig. 3. We have also plotted on the same graph results given by narrow-band model [6], which provides 12.7% of relative difference with measured end-path intensity. Following Ref. [6], at this end-path position, the sensitivity of the present model, to the number of elements is shown in Table 1, for 13, 26 and 38 elements. It can be seen that the model is almost insensitive to this number. In the table, the results obtained with the wide-band and narrow-band models [6] are also shown, the experimental value is 24.34 kW m^{-2} sr^{-1}. The inadequacy of the wide-band model can be seen. For the results presented in Fig. 3 and Table 1, using ck approach, the CPU time is about 20 s on a Sun Ultra 1 Solaris (OS 5.5) workstation. No spectral results have been provided by Ref. [6], however total or integrated intensity values are not sufficient to fully assess a spectral based model. We present in Fig. 4, for benchmark purposes, the spectral distributions of the radiative intensities at the distances of 0.066 and 1 m of the line-of-sight using 38 subdivisions. Some of the major absorption bands of H_2O
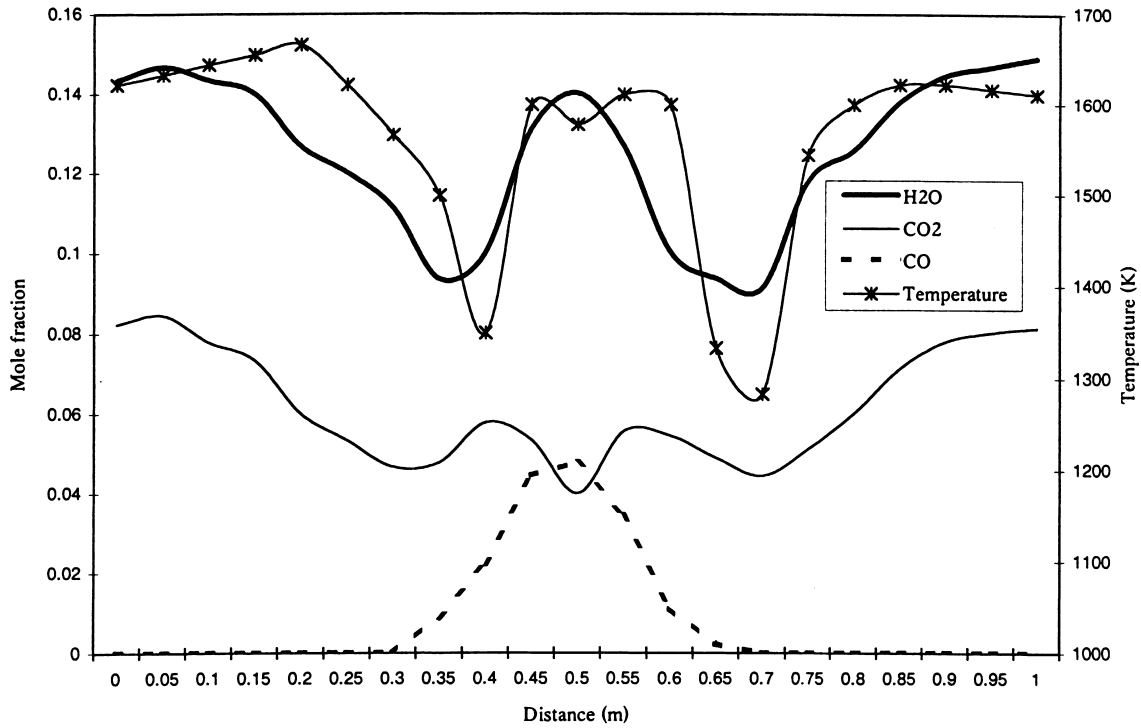
Fig. 2. Composition and temperature profiles measured within the natural gas flame at 0.6 m from burner exit — chamber pressure 10^5 Pa [6].

(1.4, 1.9, 2.7, 6.3 μm), CO_2 (2.7, 4.3, 15 μm) and CO (4.7, 2.4 μm) can be observed here.

Line-of-sight calculations are now performed, taking into account the soot contribution. The experimental concentration and temperature profiles, taken from Ref. [6], are shown in Fig. 5. The measurements were carried out at a distance of 1.3m from the burner exit in conditions similar to those of Fig. 2. The comparison results between the model predictions and the measured total radiative intensities are presented in Fig. 6. The relative differences between the predicted and measured intensities vary from about 9.5% at the position of 0.06 m to 10% at the end-path $x = 1$m. The two curves show a relatively good agreement between the calculated and experimental values. This

result underlines the ability of the presented formulation, to take into account the soot properties, in addition to the gaseous ones.

3.2. Radiative heat flux and source term calculations

Although some works in the literature have claimed accuracy of simplified models, based only on line-of-sight calculations [10,24] such calculations are not sufficient to assess a model. This is due to the fact that the major radiative quantities of interest are the heat flux and its derivative, the radiative source term, used for CFD calculations in the energy equation. To fully assess a model, one should conduct these fluxes calculations by taking

Table 1
Calculated radiation intensity at end-path (kW m^{-2} sr^{-1}) for different numbers of elements — distance from burner exit 0.6 m (experimental value = 24.22 kW m^{-2} sr^{-1})

Number of elements	Wide-band model [6]	Modified-wide band model [6]	Narrow-band model [6]	Present work (*ck* approach)
13	23.69	27.24	27.87	22.85
26	22.39	27.63	27.60	23.11
38	19.77	25.53	27.30	23.18
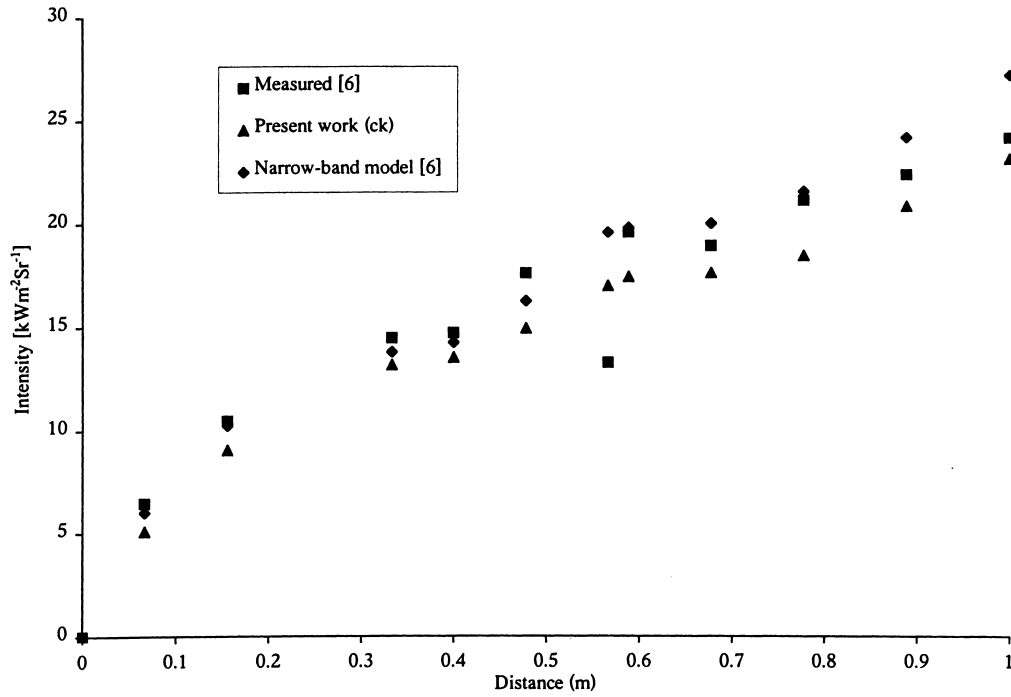
Fig. 3. Comparison of the calculated and measured radiation intensities for a natural gas flame — distance from burner exit 0.6 m.
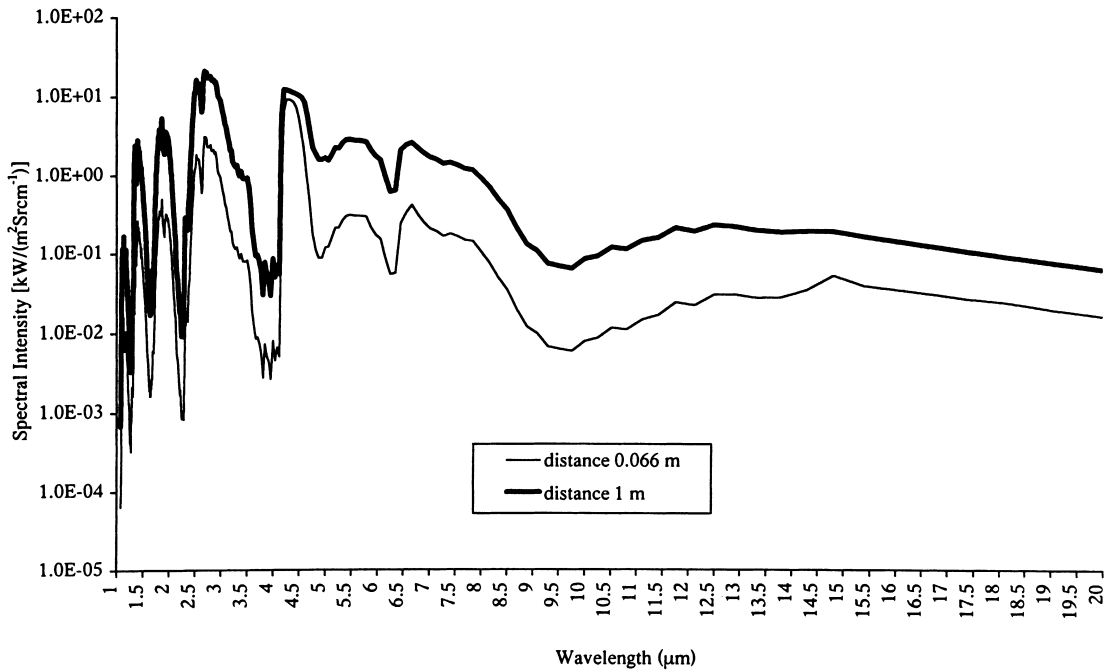
Fig. 4. Calculated spectral intensity distribution at the positions 0.066 m and 1 m.
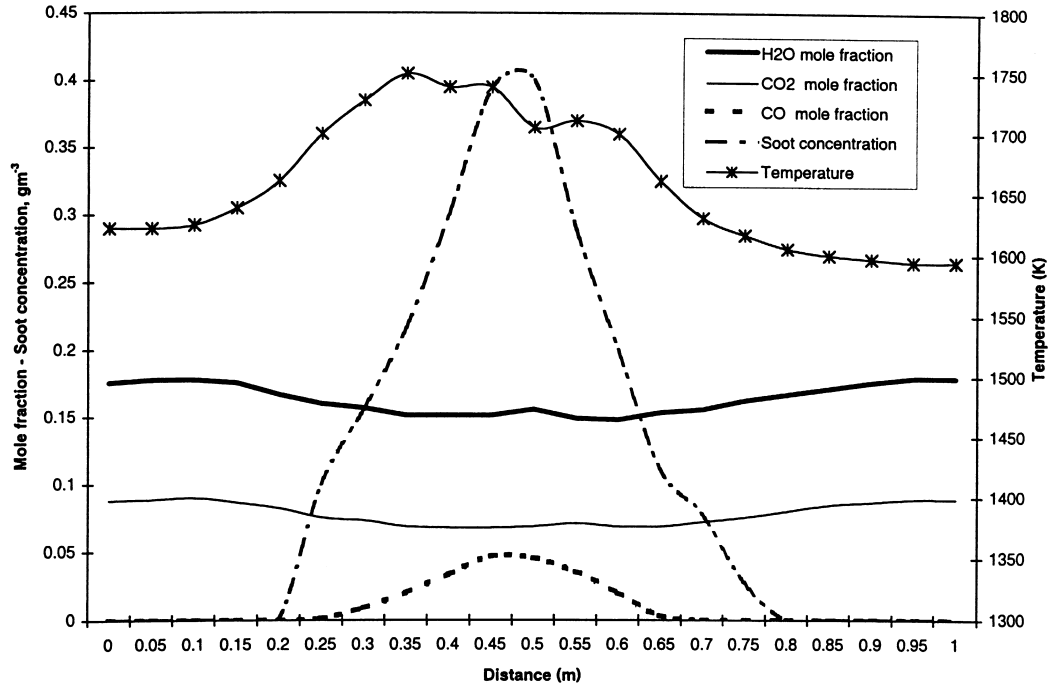
Fig. 5. Composition, soot concentration and temperature profiles measured with the natural gas flame at 1.3 m from the burner exit — chamber pressure 10^5 Pa [6].
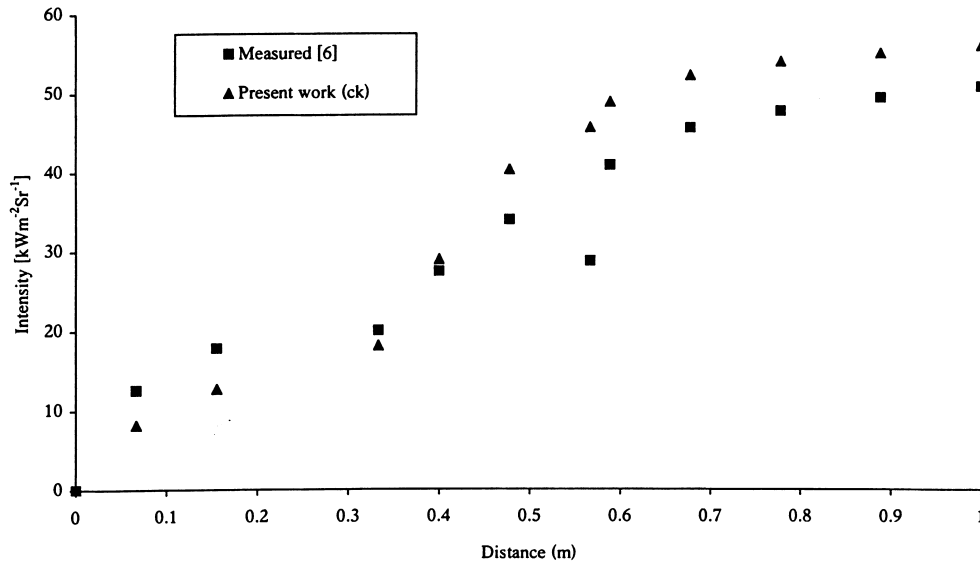
Fig. 6. Comparison of the calculated and measured radiation intensities for a natural gas flame — distance from burner exit 1.3 m.

into account the contribution of the intensities from all directions in the space (Eqs. (20)–(21)) and not from only one direction, i.e. a line-of-sight. For this purpose, the model presented in this work is analysed by comparing its results to simulated radiative source term in a one-dimensional planar slab. Predicted values of the divergence of the radiative flux $-$ dq/dx, obtained by our approach are compared with those of Menart and Lee [30]. The configuration considered is a participating medium between two parallel, reflecting/absorbing boundaries (Fig. 1). A non-scattering mixture of H_2O/N_2 medium, non-homogeneous i.e. parabolic water vapour concentration profile and non-isothermal, i.e. parabolic like temperature profile are considered. Fig. 7 shows the temperature profile. The maximum temperature is 1110 K at the centreline and 400 K at the boundaries [30]. The parabolic H_2O concentration profile is prescribed by $\chi_{H_2O} = 1 - (\frac{x}{L} - 0.5)^2/0.25$ at 1 atm total pressure. For calculations with our *ck*-based approach, 20 uniform control volumes are taken in x direction for the spatial discretization scheme. For the discrete ordinates method, 20 Gauss–Legendre quadrature points are used and radiative properties are calculated at the central point of the control volume. All the water vapour main absorption bands, ranging from 150 to 9300 cm^{-1} are considered (367 spectral bands). Results are presented in terms of total volumetric radiative source distribution ($-$dq/dx,) in Fig. 8.

The simulated results of Menart and Lee [30] are obtained with a flux technique by expansion of intensities in series (third order truncation). These authors used a NBS model and Curtis–Godson approximation for this non-homogeneous, non-isothermal and non-scattering gas case. The purpose is not to show the superiority of one approach over the other for this gaseous configuration but to show the relative tendencies of both models for heat flux predictions. Our approach can be applied to scattering problems, in contrary to the formulation presented by Menart and Lee [30]. Fig. 8 shows the relative good agreement in the whole x/L domain, between the 10 points *ck*-based approach used in our work and the simulated data of Menart and Lee [30]. In all the central region, the relative difference is about 4% between the two sets of data. Close to the boundaries, the difference is quite large, however correlated approaches are known to better predict wall correlations than NBS models (Menart et al. [31]). Moreover, even if the two programs were run on different computers, it is important to note that the CPU time on a Sun Ultra 1 workstation for this configuration with our *ck*-based approach is about 150 s. The simulations of Menart and Lee [30] has required more than 200 s on a Cray-YMP supercomputer. These results demonstrate the relatively good accuracy of the current approach and its reasonable CPU time for heat flux calculations.
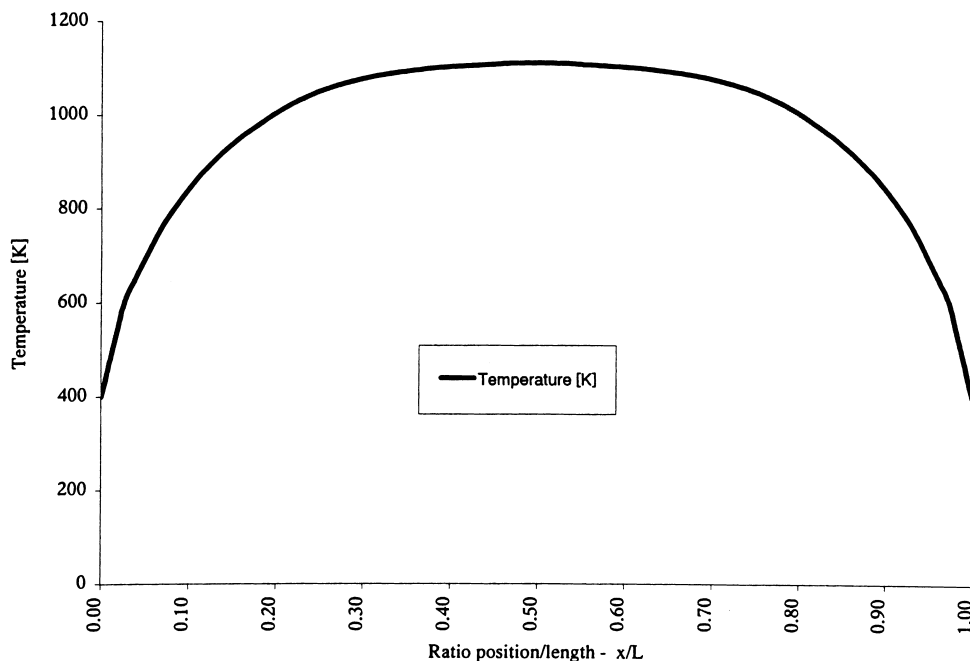
Fig. 7. The parabolic temperature profile simulated.
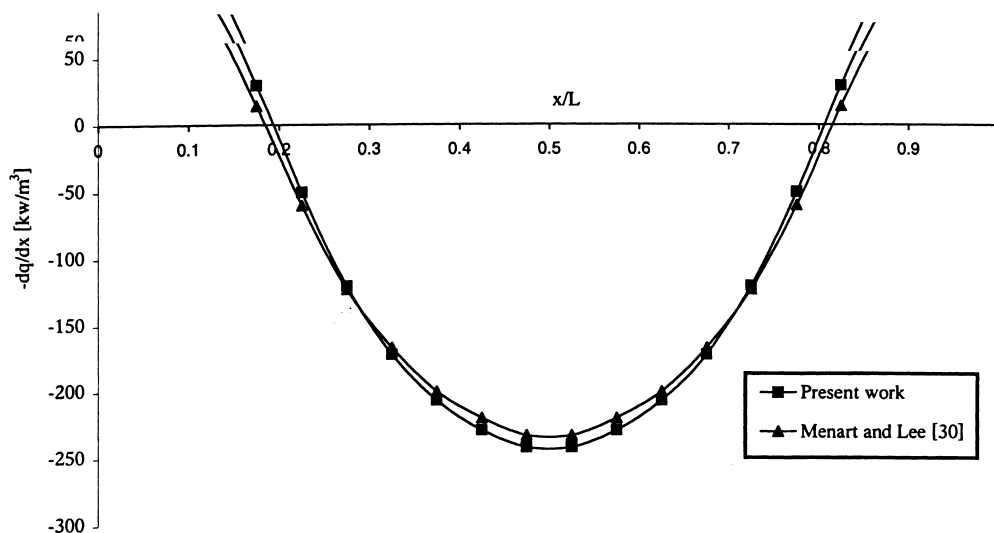
Fig. 8. Radiative source distributions for the parabolic-like temperature profile, parabolic H_2O concentration profile, boundaries reflectivities $\varrho_1 = \varrho_2 = 0.9$ (emissivities $\varepsilon^1 = \varepsilon^2 = 0.1$), $L = 10$ cm.

4. Conclusions

Radiative heat transfer in non-isothermal, non-homogeneous combustion products has been analysed. Previous modelling of the complex spectral nature of absorbing/emitting gases has been reviewed. The spectrally based formulation presented in this work, presents a way of modelling such mixtures of scattering/absorbing particles and gases, with reasonable CPU times. Application of the model to predict intensities for a natural gas flame condition, and radiative source terms for absorbing/reflecting boundary problems, has shown good agreements with the experimental measurements and benchmark data. Beyond intensities and heat fluxes calculations in fires and combustion systems, the model presented can be used to generate benchmark solutions for testing simplified models used in investigating radiative transfer in non-homogeneous and non-isothermal combustion products. Work is continuing to couple this model with the CFD code SOFIE (Simulation of Fires in Enclosures, Lewis et al. [32]) to investigate a wide range of pool fires and combustion systems configurations. CFD calculations will provide the concentrations of species and temperature spatial distributions, which are the important parameters for the radiative heat transfer analysis. For this purpose, computations using the ck-based approach will be faster by tabulating the pre-computed values of the re-ordered absorption coefficient with an interpolation procedure.

Acknowledgements

References

[1] V.I. Blinov, G.N. Khudiakov, Certain laws governing the diffusive burning of liquids, Doklady Academiia Nauk SSSR 113 (1957) 1094–1098.

[2] H.C. Hottel, Review: certain laws governing diffusive burning of liquids by V. I. Blinov and G. N. Khudiakov, Fire Research Abstracts and Reviews 1 (1958) 41–44.

[3] V. Babrauskas, Estimating large pool fire burning rates, Fire Technology 19 (1983) 251–261.

[4] T.A. Modak, The burning of large pool fires, Fire Safety Journal 3 (1981) 177–184.

[5] D.K. Edwards, Molecular gas band radiation, in: T.F. Irvine, J.P. Hartnett (Eds.), Advances in Heat Transfer, vol. 12, Academic Press, New York, 1976, pp. 115–193.

[6] W. Komornicki, J. Tomeczek, Modification of the wide band gas radiation model for flame calculation, Int. J. Heat Mass Transfer 35 (1992) 1667–1672.

[7] H.C. Hottel, A.F. Sarofim, Radiative Transfer, McGraw-Hill, New York, 1967.

[8] R.M. Goody, Y.L. Yung, Atmospheric Radiation, Oxford University Press, New York, 1989.

[9] W. Malkmus, Random Lorentz band model with exponential-tailed S^{-1} line-intensity distribution function, J. of the Optical Society of America 57 (1967) 323–329.

[10] Z. Yan, G. Holmstedt, Fast narrow-band computer

model for radiation calculations, Numerical Heat Transfer 31 (1997) 61–71.

[11] S.J. Young, Nonisothermal band model theory, J. Quant. Spectrosc. Radiat. Transfer 18 (1977) 1–28.

[12] S. Dembele, A. Delmas, J.F. Sacadura, A method for modeling the mitigation of hazardous fire thermal radiation by water spray curtains, ASME J. Heat Transfer 119 (1997) 746–753.

[13] M.Q. Brewster, Thermal Radiative Transfer and Properties, John Wiley & Sons, New York, 1992.

[14] G.L. Hubbard, C.L. Tien, Infrared mean absorption coefficients of luminous flames and smoke, J. Heat Transfer 100 (1978) 235–239.

[15] R. Longenbaugh, L. Matthews, Radiation transport in sooty pool fires: measurement and analysis, J. Quant. Spectrosc. Radiat. Transfer 47 (1992) 421–429.

[16] Z.X. Wang, in: A three layer model for oil tank fires, Second Int. Symp. on Fire Safety Science, New York, 1988, pp. 209–220.

[17] M.N. Özisik, Radiative Transfer and Interactions with Conduction and Convection, John Wiley & Sons, New York, 1967.

[18] C.F. Bohren, D.R. Huffman, Absorption and Scattering of Light by Small particles, John Wiley and Sons, New York, 1983.

[19] S.C. Lee, C.L. Tien, Optical constants of soot in hydrocarbon flames, in: Eighteenth Symposium (International) on Combustion, The Combustion Institute, Pittsburgh, 1981, pp. 1159–1166.

[20] S. Chandrasekar, Radiative Transfer, Dover, New York, 1960.

[21] B.G. Carlson, K.D. Lathrop, in: H. Greenspan, C.N. Kelber, D. Okrent (Eds.), Computings Methods in Reactor Physics, Gordon & Breach, New York, 1968, pp. 171–266.

[22] N. Selçuk, N. Kayakol, Evaluation of discrete ordinates method for radiative transfer in rectangular furnaces, Int. J. Heat Mass Transfer 40 (1997) 213–222.

[23] W.A. Fiveland, Discrete ordinates methods for radiative heat transfer in isotropically and anisotropically scattering media, ASME J. Heat Transfer 109 (1987) 809–812.

[24] L.W. Grosshandler, Radiative heat transfer in non-homogeneous gases: a simplified approach, Int. J. Heat Mass Transfer 23 (1980) 1447–1459.

[25] A.A. Lacis, V.A. Oinas, A description of the correlated k distribution method for modeling nongray gaseous absorption, thermal emission, and multiple scattering in vertically inhomogeneous atmospheres, Journal of Geophysical Research 96 (1991) 9027–9063.

[26] G.A. Domoto, Frequency integration for radiative transfer problems involving homogeneous non-gray gases: the inverse transmission function, J. Quant. Spectrosc. Radiat. Transfer 14 (1974) 935–942.

[27] A. Soufiani, J. Taine, High temperature gas radiative property parameters of statistical narrow-band model for H_2O, CO_2, CO, and correlated-k model for H_2O and CO_2, Int. J. Heat Mass Transfer 40 (1997) 987–991.

[28] W.H. Press, S.A. Teukolsky, W.T. Vetterling, B.P. Flannery, Numerical Recipes in Fortran, Cambridge Univ. Press, USA, 1992.

[29] Fiveland, W.A. A discrete ordinates method for predicting heat transfer in axisymmetric enclosures, ASME Paper 82-HT-20, 1982.

[30] J.A. Menart, H.S. Lee, Nongray gas analyses for reflecting walls utilising a flux technique, ASME J. Heat Transfer 115 (1993) 645–652.

[31] J.A. Menart, H.S. Lee, T.K. Kim, Discrete ordinates solutions of nongray radiative transfer with diffusely reflecting walls, ASME J. Heat Transfer 115 (1993) 184–193.

[32] M.J. Lewis, M.B. Moss, P.A. Rubini, CFD coupling of combustion and heat transfer in compartment fires, in: Fifth Int. Sympos, Fire Safety Science, 1997, pp. 463–474.